lubricants

MDPI

Article

Wear and Friction Behavior of Cellulose Nanofibers-Based Biogreases

Claudia Roman [1], Miguel Ángel Delgado Canto [1,*], María García-Pérez [1], Samuel D. Fernández-Silva [1], Ke Li [2] and Moisés García-Morales [1]

[1] Departamento de Ingeniería Química, Centro de Investigación en Tecnología de Productos y Procesos Químicos (Pro2TecS), Campus de "El Carmen", Universidad de Huelva, 21071 Huelva, Spain; claudia.roman@diq.uhu.es (C.R.); maria.gperez@diq.uhu.es (M.G.-P.); samuel.fernandez@diq.uhu.es (S.D.F.-S.); moises.garcia@diq.uhu.es (M.G.-M.)

[2] School of Transportation and Logistics Engineering, Wuhan University of Technology, Wuhan 430063, China; li_ke@whut.edu.cn

* Correspondence: miguel.delgado@diq.uhu.es

Abstract

(1) Background: Developing fully bio-based lubricating greases requires eco-friendly alternatives to conventional harmful components. This study highlights unmodified nanocellulose as an effective structuring agent in vegetable oils, enabling 100% bio-based formulations. (2) Methods: Three bio-based greases were formulated using 1.4 wt.% cellulose nanofibers (CNFs), derived from elm wood pulp through mechanical and chemical pretreatment, as thickening agents in castor oil. Their tribological performance was evaluated under varying temperatures and contact loads and compared to a reference lithium-based grease (LBG) containing 14 wt.% thickener, also formulated with castor oil. (3) Results: Among the CNFs, the unbleached variant (CNF-U) which retained the highest lignin content exhibited the highest coefficient of friction (COF), ranging from 0.09 to 0.14 across test conditions, along with a wear scar diameter of approximately 615 µm at 60 °C. Notable differences in shear stress sensitivity were observed between mechanically and chemically treated nanofibers. The TEMPO-oxidized nanofiber (CNF-TO) grease demonstrated outstanding lubrication stability across contact loads of 10–40 N and temperatures from 25 to 100 °C, maintaining COF values below 0.1—comparable to the reference LBG at 40 N load. Wear scar analysis confirmed that CNF-based greases significantly reduced wear relative to the lithium reference: CNF-B produced the smallest scar diameter (188 µm at 25 °C) while CNF-TO yielded the lowest at 60 °C (457 µm). (4) Conclusions: Nanofiber type and pretreatment significantly impact the tribological performance of CNF-based biogreases. TEMPO-oxidized CNFs provided stable lubrication under varied loads and temperatures, while all CNFs showed strong thermal adaptability, supporting their use in sustainable lubrication.

Keywords: friction; wear; cellulose nanofiber; biogreases; environmentally acceptable lubricant

Received: 21 July 2025
Revised: 9 September 2025
Accepted: 18 September 2025
Published: 20 September 2025

Citation: Roman, C.; Delgado Canto, M.Á.; García-Pérez, M.; Fernández-Silva, S.D.; Li, K.; García-Morales, M. Wear and Friction Behavior of Cellulose Nanofibers-Based Biogreases. *Lubricants* **2025**, *13*, 423. https://doi.org/10.3390/lubricants13090423

1. Introduction

The lubricant industry is under growing pressure to replace traditional greases formulated with lithium soaps and mineral base oils, driven by both supply limitations and increasingly stringent environmental regulations. Lithium, designated as a critical raw material by the European Union, is not only costly but also scarce, underscoring the urgency of developing lithium-free alternatives. Additionally, the projected depletion of fossil oil reserves further emphasizes the need for sustainable solutions, while

regulatory frameworks—such as the U.S. Vessel General Permit (VGP) and the EU Green Deal—mandate that lubricants used in environmentally sensitive applications (e.g., marine, wind energy) be biodegradable, non-toxic, and bio-based. This shift is propelling research and manufacturing toward practices that align with the principles of environmental stewardship and resource efficiency, as outlined in the United Nations Sustainable Development Goals (SDGs), including SDG 7 (Affordable and Clean Energy), SDG 12 (Responsible Consumption and Production), and SDG 13 (Climate Action). Nevertheless, many commercial biogreases still rely on synthetic esters or require chemical modifications that elevate production costs and environmental impact.

In particular, the lubricant market faces significant challenges regarding the environmental consequences of lubricant use in sensitive sectors such as maritime operations, wind energy production, and agriculture. Wind turbines, for instance, depend on environmentally acceptable lubricants (EALs) for critical components like gearboxes, bearings, and hydraulic systems. EU-specific regulations, such as the Wind Power Package introduced in 2023, emphasize the importance of sustainable materials and practices to meet environmental standards and reduce the ecological footprint of wind energy projects. Similarly, EALs are widely used in marine vessel components, including stern tubes, thrusters, and hydraulic systems [1]. The Vessel General Permit (VGP), issued by the U.S. Environmental Protection Agency, governs incidental discharges in U.S. waters and stipulates the use of EALs in designated applications to mitigate environmental harm.

In recent years, significant research efforts have focused on developing EALs utilizing vegetable oils and biodegradable thickeners. To qualify as an EAL, a lubricant must be formulated from renewable, biodegradable, low-toxicity, and non-bioaccumulative materials that pose minimal risk to biodiversity, thereby reducing overall environmental impact [1]. Achieving this requires balancing ecological responsibility with high industrial performance. Common base oils used in EAL formulations include vegetable oils, synthetic esters, low molecular weight polyalphaolefins (e.g., PAO4 and PAO6, with kinematic viscosities, at 100 °C, of 4 and 6 cSt, respectively) [2] and polyalkylene glycols (with molecular weights higher than 1500 g/mol) [3]. However, evolving environmental regulations are increasingly mandating the use of nearly fully bio-based lubricants, particularly in applications where the risk of environmental contamination is high. This presents a notable challenge for grease formulations, as the thickening agent—typically a metallic soap—can constitute up to 20 wt.% of the product, complicating efforts to meet bio-based criteria.

Numerous studies have investigated starches, modified polysaccharides, and lignocellulosic derivatives as potential alternatives to metallic soaps [4–8]. However, many of these materials require complex functionalization processes, which can undermine their sustainability. Among emerging candidates, lignocellulosic materials stand out for their renewability, mechanical strength, and ability to form three-dimensional entangled networks suitable for grease structuring [4,5]. Despite their advantages, incorporating lignocellulosic materials into non-polar base oils remains challenging due to their inherently hydrophilic nature. This leads to aggregation and the formation of agglomerates, which eventually settle and cause sedimentation over time. To overcome these limitations, many studies have focused on using functionalized derivatives [6–8]. Nevertheless, such approaches often result in higher manufacturing costs and increased environmental impact.

In this context, the use of unmodified cellulosic materials remains relatively underexplored. Taha et al. [9] demonstrated that incorporating 2 wt.% cellulose nanofiber (CNF) into spent engine oil 10W30 led to a 14.5% increase in kinematic viscosity and a 31% reduction in wear scar width. Similarly, Awang et al. [10] identified an optimal concentration of 0.1 wt.% cellulose nanocrystals (CNC) in SAE 40 base oil, achieving notable improvements in viscosity index and storage stability. Li et al. [11] explored CNC as an eco-

friendly additive in lithium-based greases, reporting reductions in friction and wear of up to 16 and 29%, respectively. These enhancements were attributed to surface mending and protective effects, combined with the strong hydrodynamic behavior of the highly viscous base oil (220 cSt at 40 °C). More sustainable alternatives have also emerged. Ilyin et al. [12] demonstrated that dispersions of microfibrillated cellulose in triethyl citrate show strong potential as biodegradable greases, exhibiting effective performance even at extremely low temperatures (down to −50 °C). Semi-dilute (1 wt.%) dispersions reduce wear by filling surface imperfections, while concentrated (7 wt.%) suspensions form tribofilms that lower friction. Guimarey et al. [13] examined the use of cellulose nanocrystals (CNCs) as lubricant additives in isopropyl palmitate (IPP) oil to enhance tribological behavior. Their findings revealed that CNC/IPP nanolubricants significantly improved friction reduction and wear resistance with as little as 0.25 wt.% CNC. However, CNC concentrations exceeding 0.5 wt.% resulted in agglomeration and thermal instability above 60 °C, leading to a 25–30% increase in the coefficient of friction [13]. These tribological improvements contribute to extended lubricant and machinery service life, while also offering notable environmental advantages.

In this experimental study, we begin with the hypothesis that cellulose nanofibers (CNFs), even at low concentrations, can offer thickening and lubrication performance comparable to traditional lithium soap-based thickeners in castor oil. While previous research has highlighted the tribological advantages of cellulose nanocrystals and microfibrillated cellulose as additives, the impact of nanofiber origin (bleached vs. unbleached) and pretreatment method (mechanical vs. chemical) on tribological properties remains insufficiently explored. We further hypothesize that the pretreatment and chemical modification of cellulose significantly influence the rheological and tribological behavior of biogreases. The potential of unmodified or minimally processed CNFs to form stable, high-performance biogreases—particularly under varying mechanical loads and temperature conditions—has yet to be fully addressed. To mitigate the challenges posed by CNFs' highly hydrophilic nature, a solvent exchange strategy has been employed, enabling better integration of CNFs into vegetable oil matrices. This approach has resulted in enhanced storage stability and rheological performance, positioning CNF-based formulations as a promising and sustainable alternative to conventional lubricating greases [14,15]. Despite encouraging preliminary findings, tribological research in this domain remains limited. There is considerable scope for further investigation, including a deeper understanding of the molecular mechanisms governing friction behavior and the development of scalable production methods for nanocellulose-based biogreases.

In this context of sustainable development and transition to a circular economy, this study aims to evaluate the tribological performance of biogreases formulated with just 1.4 wt.% of cellulose nanofibers—subjected to both mechanical and chemical treatments—as the sole thickening agent in castor oil. The investigation spans a broad range of temperatures, normal loads, and sliding velocities to assess their practical viability. This work represents a foundational step toward developing a new class of environmentally acceptable lubricating greases. The novelty of this approach lies in the use of non-chemically modified cellulose nanofibers as a thickener, offering a sustainable alternative to conventional formulations. These biogreases have the potential to meet growing market demands for eco-friendly lubricants, particularly in applications where environmental contamination from lubricant leakage is a critical concern. By providing robust performance and improved environmental compatibility, these formulations present a promising solution for industrial use.

2. Materials and Methods

2.1. Raw Materials

Castor oil, provided by Guinama (Spain), was selected as the base oil. It has a kinematic viscosity of 242.5 cSt at 40 °C. Three distinct types of cellulose nanofibers derived from elm wood pulps were supplied by the National Institute of Agricultural and Food Research and Technology, INIA-CSIC, in Madrid (Spain). In the first two types, bleached and unbleached elm kraft pulps were submitted to mechanical pretreatment, consisting in refining in a standard laboratory PFI mill, before their final microfluidization. These nanofibers are hereinafter referred to as CNF-B and CNF-U, for bleached and unbleached (with a total lignin content of ~2.6 wt.%) pulps, respectively. For the third type, the bleached elm pulp was subjected to TEMPO (2,2,6,6-tetramethylpiperidine-1-oxyl)-mediated oxidation before its microfluidization. This nanofiber is hereinafter referred to as CNF-TO. Details of their production and characterization are available in Roman et al. [14]. All these cellulose nanofibers were provided as never-dried gel-like aqueous suspensions with a solid content of approximately 2 wt.%.

2.2. Biogreases Preparation

The incorporation of gel-like aqueous suspensions of different CNFs into castor oil was achieved through a solvent exchange method utilizing methanol, as previously detailed in Roman et al. [14]. This method efficiently integrates CNFs into the vegetable oil, yielding homogeneous and storage-stable dispersions and, thereby, enhancing the rheological and tribological properties of the biogrease. A low nanofiber concentration of 1.4 wt.% was used, based on its ability to form a skeleton similar to traditional lithium greases, yielding homogeneous and stable formulations with noticeable pseudoplastic behavior. These biogreases showed penetration values equivalent to a 00 NLGI grade, based on one-quarter-scale penetration measurements as specified in ASTM D217. As a benchmark, a lubricating grease containing 14 wt.% lithium soap (ten times the nanofiber concentration) in castor oil was prepared, following the procedure outlined in Delgado et al. [16]. It is worth pointing out that lithium greases are excellent for challenging metal-to-metal heavy-load applications. Hence, this formulation, using the same base oil, enabled a comparative evaluation with respect to a traditional metal soap thickener at its typical concentration.

2.3. Biogreases Characterization

In the context of tribological characterization, both the coefficient of friction (COF) and wear scar diameter were analyzed. A ball-on-three-plates tribology cell (Figure 1c) was employed, coupled to a Physica MCR 501 controlled stress rheometer (Figure 1a) from Anton Paar (Graz, Austria). The tribology cell consisted of a lower section featuring three 45–pitched steel plates (C45E-1.1191) with a hardness rating of 25–30 HRC. The upper section was designed to hold a fixed bearing ball made of chrome steel (100Cr6) with a diameter of 12.7 mm [17]. The plates and ball were securely fixed in their respective geometries to prevent any unwanted vibrations or rolling, thereby enabling the tests to be conducted under pure sliding. The coefficient of friction was calculated as the ratio of the measured friction force to the applied normal load on the three plates.

The evolution of the coefficient of friction was monitored across a rotational speed range of 0.1 to 1000 rpm, corresponding to sliding velocities of 0.047 to 470.2 mm/s. The tests were conducted at contact loads of 10, 20, and 40 N for a selected temperature of 25 °C, and at temperatures of 25, 40, and 100 °C, for a selected load of 20 N. These temperatures were within the typical operating range of wind turbine bearings [18], a potential consumer of large amounts of these bio-based lubricating greases. Moreover, wear was evaluated at a normal load of 20 N and a constant rotational speed of 40 rpm (a sliding velocity of

18.8 mm/s) for 1800 s at 25 and 60 °C. After completing the tests, the plates were thoroughly cleaned with ethanol. Subsequently, wear scar diameters were examined using an Olympus SC50 camera mounted on a BX51 optical microscope (Olympus, Tokyo, Japan).

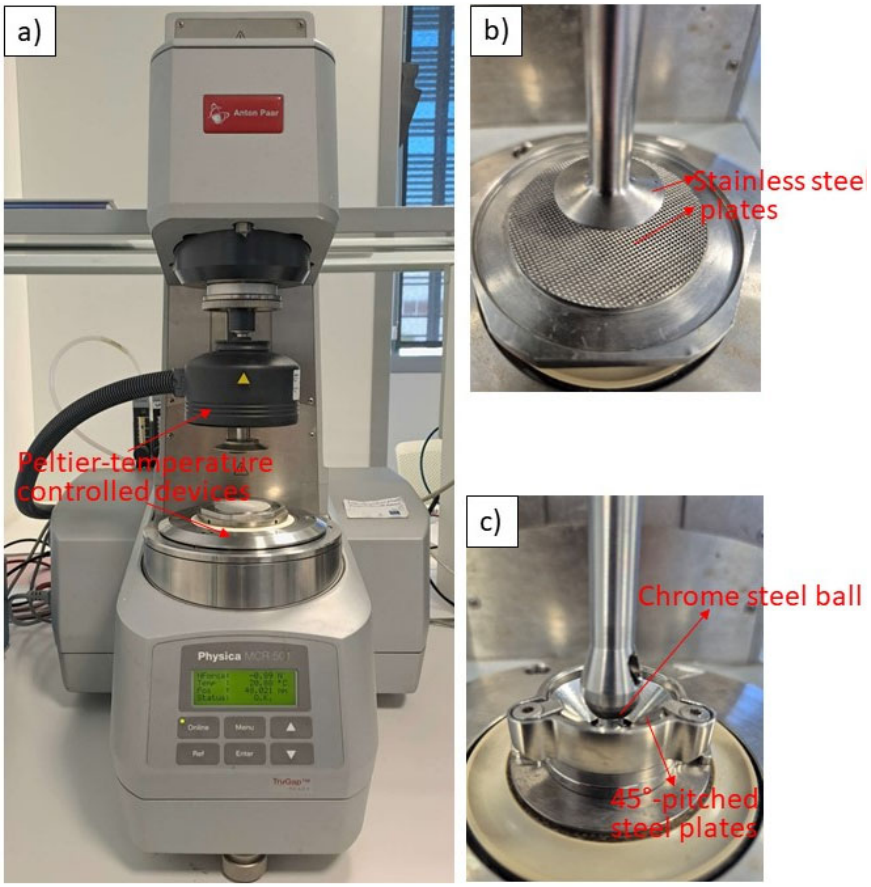

Figure 1. Experimental setup: (**a**) Physica MCR 501 controlled stress rotational rheometer; (**b**) rough plate–plate geometry; (**c**) ball-on-three-plates tribology cell.

Results from rheological tests provided a deeper understanding of the friction and wear results. Those tests were performed in a Physica MCR 301 controlled stress rheometer from Anton Paar (Graz, Austria), using a rough plate–plate geometry (25 mm diameter, 1 mm gap, Figure 1b). Steady-state viscous flow tests were carried out in a shear rate range between 10^{-2} and 10^{2} s^{-1}, at selected temperatures of 25, 40 and 100 °C. Moreover, the mechanical stability of the biogreases was evaluated under large amplitude oscillatory shear (LAOS) conditions, at 25 and 60 °C. The protocol consisted of three sequential dynamic shear time sweeps conducted at 6.28 rad/s (1 Hz), with the middle sweep being carried out at a stress beyond the linear viscoelastic (LVE) regime, and the first and last sweeps at an LVE stress. For this investigation, a non-linear stress value of 200 Pa was arbitrarily chosen and evaluated. Previously, the LVE range had been identified by performing a dynamic stress sweep test at a fixed frequency of 6.28 rad/s (1 Hz), at 25 and 60 °C. The LVE was characterized by a critical stress value below which the viscoelastic functions remained stress-independent.

At least three replicates were conducted for each operating condition and sample to ensure that the average values achieved statistical significance at the 95% confidence level.

3. Results and Discussion

3.1. Friction Behavior of Nanocellulose-Based Biogreases: Effect of Contact Load

This section, along with those that follow, presents a systematic investigation into the tribological behavior of three biogreases, each formulated with a fixed nanocellulose concentration of 1.4 wt.%. The study aims to evaluate their effectiveness in reducing friction across various lubrication regimes. For reference, neat castor oil and a lithium-based grease—formulated with castor oil and 14 wt.% lithium soap (hereafter referred to as LBG)—were included. The frictional performance of the nanocellulose-based biogreases under pure sliding conditions was assessed using Stribeck-like curves (Figures 2 and 3), which illustrate how the coefficient of friction (COF) varies with sliding velocity in lubricated contacts.

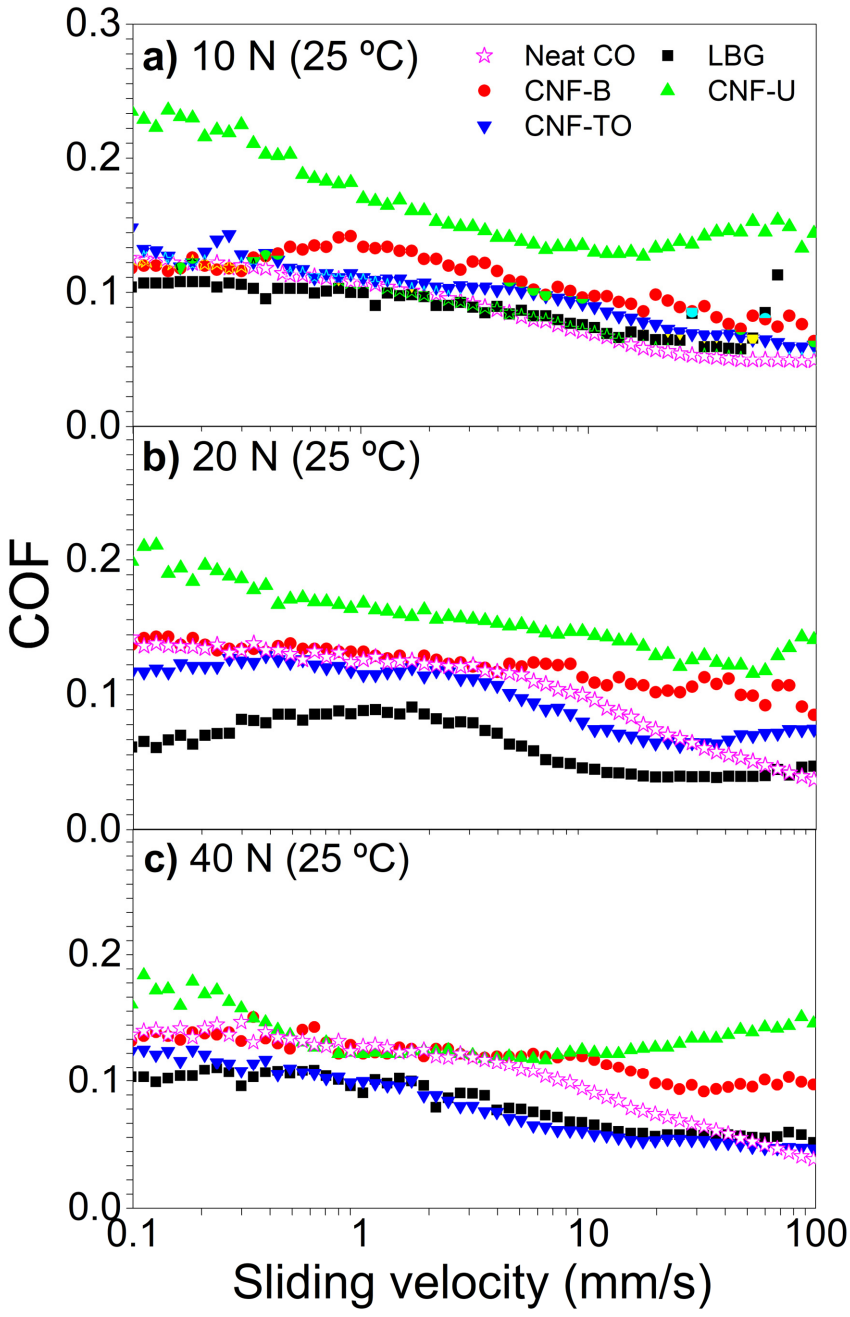

Figure 2. Stribeck-like curves for the three 1.4 wt.% CNF-based biogreases studied, at 25 °C, at selected contact loads: (**a**) 10 N; (**b**) 20 N; (**c**) 40 N. Neat castor oil (CO) and LBG (reference lithium-based grease) are included for comparison purposes.

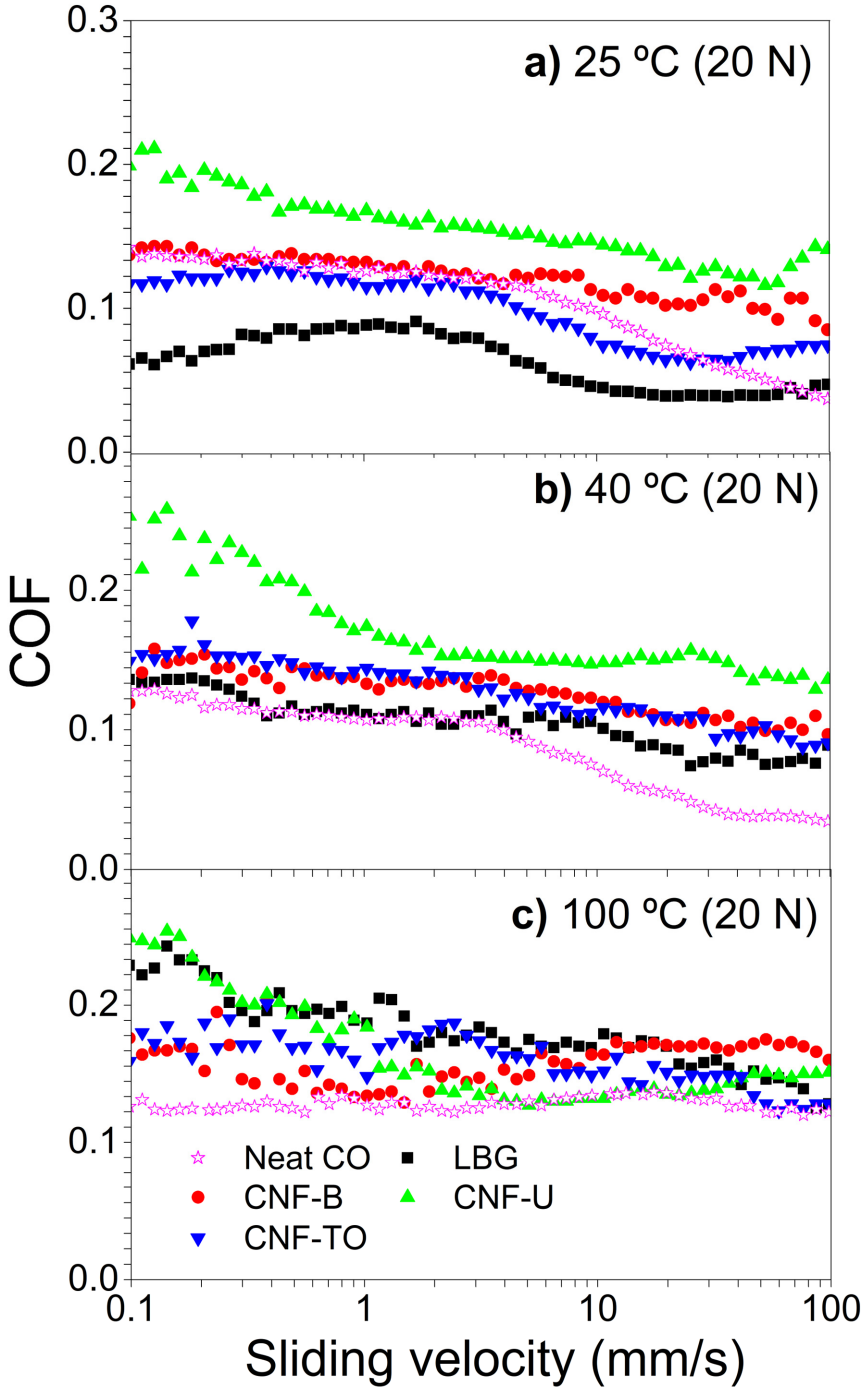

Figure 3. Stribeck-like curves for the three 1.4 wt. % CNF-based biogreases studied, at 20 N, at selected temperatures: (**a**) 25 °C; (**b**) 40 °C; (**c**) 100 °C. Neat castor oil (CO) and LBG (reference lithium-based grease) are included for comparison purposes.

In Figure 2, measurements were conducted at 25 °C under three contact loads: 10, 20, and 40 N. These conditions enabled a comprehensive evaluation of each biogrease's ability to sustain film formation and maintain lubrication efficacy under varying load severities and friction regimes. Overall, the CNF-U biogrease exhibited higher COF values than the other two formulations across all tested loads. Previous research [14] indicated that unbleached cellulose nanofibers—characterized by a high aspect ratio and residual lignin and hemicellulose—form a densely entangled network. Additionally, the unbleached pulp yielded the lowest nanofibrillation rate (50.2%), which may hinder lubricating film formation at lower sliding velocities. Conversely, the robust microstructure of the thickener

resists mechanical disruption, increasing internal friction in the hydrodynamic regime. As a result, CNF-U demonstrated consistently higher friction compared to the biogreases derived from bleached pulps. Notably, at 10 and 20 N, CNF-U maintained the highest COF values across the entire sliding velocity range. However, at 40 N, COF values decreased significantly within the mixed lubrication regime, and the minimum COF shifted toward lower sliding velocities. This behavior suggests that, under high load, the structural resistance of CNF-U may be substantially compromised during the churning phase [19], facilitating base oil release and film formation at reduced velocities. Such characteristics could be advantageous in applications where controlled friction is beneficial, such as braking systems or precision motion devices.

At 10 and 20 N, CNF-B and CNF-TO biogreases exhibited COF values comparable to castor oil under solid friction conditions. For CNF-B, friction increased at higher sliding velocities, where fluid friction dominates. In contrast, CNF-TO displayed Stribeck-like curves closely resembling those of the reference LBG, with COF values consistently below 0.1 and significantly lower than castor oil—particularly at 40 N. This suggests that CNF-TO may be well-suited for metal-to-metal, heavy-load applications. The tribological performance of CNF-TO extended beyond the boundary regime into higher sliding velocities, where a thin lubricant film likely forms under mixed friction conditions. This film reduces asperity contact and gradually lowers friction. The enhanced behavior may be attributed to TEMPO-mediated oxidation, which increases the nanofibers' surface charge (Z-potential of −68.1 mV, compared to −28.4 mV for CNF-B) and alters their morphology [15]. These changes appear to improve compatibility with castor oil and overall lubrication performance.

In summary, the frictional response of CNF-based biogreases was strongly influenced by the applied load. CNF-U consistently exhibited higher COF values due to its dense, lignin-rich structure, while CNF-B and CNF-TO provided lower friction, particularly under higher loads. Among them, CNF-TO demonstrated behavior most similar to lithium grease, underscoring its potential for demanding, heavy-load applications.

3.2. Friction Behavior of Nanocellulose-Based Biogreases: Effect of Temperature

The most pronounced differences in the friction behavior of the biogreases studied were observed at a load of 20 N. Consequently, this load was selected for evaluating the effect of temperature. The temperatures chosen for this investigation (25, 40, and 100 °C) span from ambient to elevated conditions that simulate demanding operational environments, such as those found in wind turbine bearings [20]. Notably, testing at 100 °C is essential for assessing the thermal stability and performance limits of these biogreases, thereby ensuring their reliability under high-temperature working conditions.

Stribeck-like curves for all biogreases at 25, 40, and 100 °C are presented in Figure 3. At 25 °C (Figure 3a), a distinct difference in the coefficient of friction (COF) is evident between the CNF-based biogreases and the reference lithium grease at 20 N. However, these differences diminish as the temperature increases (Figure 3b,c), with all friction curves progressively flattening at higher temperatures [21]. It is worth noting that the reference lithium-based grease (LBG) at 25 °C exhibits a characteristic "bump" in the boundary lubrication regime—where the COF initially rises with sliding velocity to a local maximum before decreasing as fluid friction surpasses solid friction. This phenomenon is referred to as "inverse-Stribeck" behavior [22]. Additionally, the reference LBG demonstrates a significantly lower COF compared to neat castor oil at 25 °C, indicating superior lubrication performance. This improvement is attributed to the enhanced consistency provided by 14 wt.% lithium soap, which facilitates better separation of the frictional surfaces. As highlighted by Wang et al. [23], the consistency of lithium grease influences COF through

its impact on structural strength and film-forming capability. Consequently, the reference LBG shows greater efficiency in maintaining and replenishing the lubrication film than neat castor oil under ambient conditions.

The CNF-based biogreases exhibited higher coefficients of friction (COF) compared to the reference lithium-based grease (LBG). Among them, only the CNF-TO biogrease showed slightly lower COF values than neat castor oil at 25 °C, in both boundary and mixed lubrication regimes. Notably, this formulation also displayed a subtle "bump" in the boundary regime, similar to the behavior observed with LBG. A further reduction in friction was observed as sliding velocity was increased, marking the transition from boundary to mixed lubrication, where both surface asperities and the lubricant film share the load [24]. The enhanced lubrication efficiency of CNF-TO relative to the other biogreases may be attributed to improved alignment or distribution of its nanofibers within the lubricant film, as demonstrated in our previous work [14]. This structural organization likely contributed to its superior friction-reducing capability. It is also noteworthy that CNF-TO reached its minimum COF at sliding velocities comparable to those of the reference LBG. In conclusion, these findings highlight the exceptional potential of CNF-TO as a structuring agent in castor oil, delivering optimal tribological performance across various lubrication regimes at 25 °C and 20 N.

Instead, the coefficient of friction (COF) values for CNF-B and CNF-U biogreases remained nearly constant or exhibited a slight decline across the entire range of sliding velocities studied. As discussed later, cellulose nanofibers derived from PFI refining—a physical pre-treatment method—such as CNF-B and CNF-U, produced structures that were less sensitive to shear stress. This characteristic likely limits their oil bleeding capacity compared to cellulose nanofibers obtained via chemical TEMPO-mediated oxidation, such as CNF-TO. Notably, CNF-U biogrease consistently exhibited the highest COF values throughout the sliding speed range. This behavior may be attributed to its denser, more entangled network, which contains a higher concentration of residual lignin and other natural components inherent to the unbleached CNF elm pulp. At higher sliding velocities, CNF-U biogrease showed a marked increase in COF, suggesting a breakdown in its load-carrying capacity and the onset of starved lubrication.

When the temperature was raised to 40 °C, the frictional behavior of the reference lithium-based grease (LBG) changed significantly, aligning more closely with that of CNF-TO and CNF-B biogreases. At this temperature, CNF-TO and CNF-B displayed nearly identical friction profiles, while CNF-U continued to register the highest COF values (Figure 3b). At 100 °C, castor oil's frictional performance was notably affected, maintaining nearly constant COF values even within the hydrodynamic lubrication regime. In contrast, CNF-B and CNF-TO biogreases showed only minor changes in friction behavior at this elevated temperature, closely mirroring the performance of castor oil. Conversely, the reference LBG exhibited increased COF values across all sliding velocities (Figure 3c). This convergence of Stribeck-like curves indicates that, at higher temperatures, the distinct characteristics of each grease become less influential, and lubrication behavior is primarily governed by the base oil properties. Special attention should again be given to CNF-U biogrease at 100 °C, which demonstrated a decrease in COF with increasing sliding velocity, followed by a gradual rise in friction at higher speeds. These findings suggest that the microstructure of the CNF-based thickeners under thermal and mechanical stress is more resilient than that of the reference LBG, resulting in less pronounced changes in friction behavior.

In summary, temperature had a more substantial impact on the lithium-based reference grease than on the CNF-based biogreases. CNF-TO consistently delivered superior frictional performance across lubrication regimes, while CNF-B and CNF-U exhibited

limited adaptability and higher COF values. At elevated temperatures, the friction curves of all greases tended to converge, highlighting the dominant influence of the base oil under high-temperature conditions.

3.3. Comparative Analysis of the Shear-Induced Structural Degradation of Nanocellulose-Based Biogreases

The frictional behavior of lubricating grease is influenced by the mechanical resistance of its thickener microstructure [25]. This section presents a comparative analysis of shear-induced structural degradation in nanocellulose-based biogreases, alongside the influence of temperature, in relation to the frictional behavior discussed earlier. The investigation employs a dual rheological approach, combining steady-state flow measurements with viscoelasticity tests conducted both within and beyond the linear viscoelastic range.

Figure 4 presents a comparative analysis of the steady-state viscous flow curves at 25, 40, and 100 °C for the three CNF-based biogreases. For reference, the lithium-based grease (LBG) was also included to facilitate comparison. This evaluation aims to deepen the understanding of how temperature variations influence the dynamic viscosity of CNF-based biogreases and, consequently, their shear-induced structural degradation—an important factor affecting frictional behavior. All greases examined exhibited pronounced pseudoplastic (shear-thinning) behavior, characterized by a reduction in dynamic viscosity with increasing shear rate. These findings indicate that incorporating cellulose nanofibers into castor oil produces biogreases with viscous flow characteristics comparable to conventional lithium greases, despite requiring significantly lower thickener concentrations. This underscores their efficiency and potential for reducing material usage while maintaining performance. At 25 and 40 °C, the CNF-B and CNF-U biogreases displayed viscous flow behavior similar to that of the reference LBG.

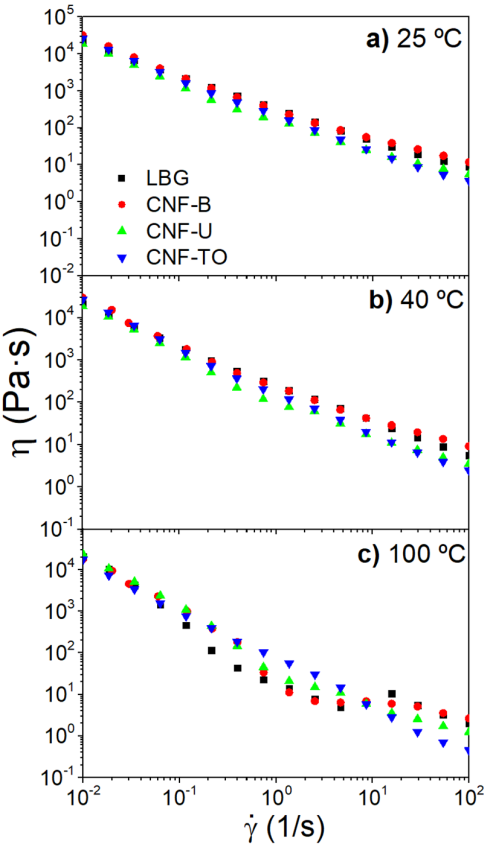

Figure 4. Viscous flow curves for the three CNF-based biogreases at: (**a**) 25 °C; (**b**) 40 °C; (**c**) 100 °C. LBG (reference lithium-based grease) is included for comparison purposes.

As expected, all biogreases exhibited a reduction in dynamic viscosity with increasing temperature, with the decline at 100 °C being particularly pronounced. This behavior is attributed to thermal weakening of the network structure, primarily caused by the breakdown of hydrogen bonds within the oleogel matrix. Notably, the sharp drop in dynamic viscosity at 100 °C and intermediate shear rates observed in CNF-B and CNF-U biogreases—as well as in the reference LBG—is especially significant. This phenomenon suggests the presence of a dynamically unstable region, likely resulting from a non-homogeneous velocity field during the viscometric flow of these complex materials [26,27]. In contrast, the CNF-TO biogrease maintained a more stable viscosity profile across the studied shear rate and temperature ranges. This observed stability indicates that the CNF-TO nanofiber formed a robust internal network structure capable of accommodating thermal variations while preserving consistent flow behavior and performance.

Furthermore, the shear-induced structural degradation of CNF-based biogreases was investigated through non-linear viscoelastic tests designed to monitor the material's response to external stress beyond the linear viscoelastic (LVE) region, as well as its ability to "heal" once the perturbation ceased. These tests aimed to provide insight into the biogreases' resistance to structural breakdown under shear and their capacity to retain mechanical stability. Figure 5 illustrates the log-linear evolution of the complex modulus $|G^*|$ over time, under constant temperature and frequency conditions. Three sequential dynamic shear time sweeps were performed: (a) an initial 5-min loading interval under stress within the LVE regime, yielding the complex modulus of the undisturbed grease, $|G_0^*|$; (b) a 30-min interval under stress exceeding the LVE limit, resulting in structural degradation and a reduced modulus, $|G_1^*|$; and (c) a final 30-min interval under the same initial stress, during which partial recovery of the grease structure was observed, yielding $|G_2^*|$.

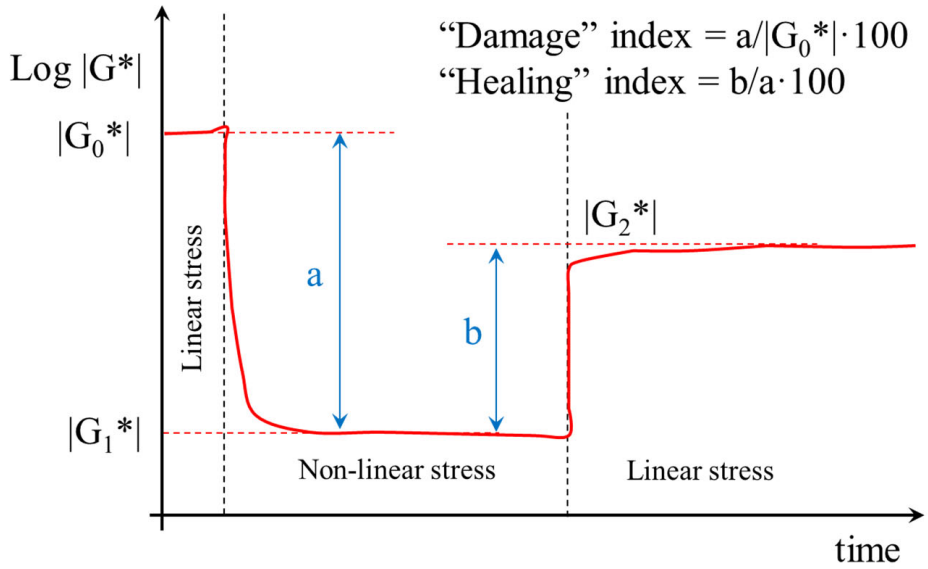

Figure 5. Schematic of the time evolution of the dynamic shear modulus, $|G^*|$, at constant temperature and frequency. Definitions of "damage" and "healing" indexes are included.

Based on the definitions provided in Figure 5, the calculated values of the "damage" and "healing" indexes for the biogreases studied are summarized in Table 1. As observed, increasing temperature generally made the biogreases more susceptible to mechanical disruption. This effect is attributed to the weakening of intermolecular interactions—such as van der Waals forces and hydrogen bonding [16]—which compromised their thickener's structural resistance. However, the extent of this behavior varied significantly depending

on the thickener used. For instance, the CNF-B biogrease exhibited a sharp rise in the "damage" index from 55.7% to 98.9% as the temperature increased from 25 to 60 °C. Similarly, the CNF-TO biogrease showed consistently high "damage" index values of 98.3 and 99.8% at 25 and 60 °C, respectively. These results closely mirror those of the reference LBG, which also experienced substantial structural breakdown at both 25 °C (95.6%) and 60 °C (99.2%). Such findings indicate that these biogreases are highly sensitive to large-amplitude strain, regardless of temperature. In contrast, the CNF-U biogrease demonstrated the greatest resistance to shear-induced structural degradation and lower sensitivity to temperature, with its "damage" index increasing modestly from 28.9 to 38.6% over the same temperature range.

Table 1. Calculated values of "damage" and "healing" indexes, and their ratios, at 25 and 60 °C, for greases which were first subjected to a non-linear stress of 200 Pa and then let recover.

Biogreases	"Damage" Index		"Healing" Index		Damage/Healing Ratio	
	25 °C	60 °C	25 °C	60 °C	25 °C	60 °C
CNF-B	55.7	98.9	52.0	31.0	1.07	3.19
CNF-U	28.9	38.6	90.3	78.5	0.32	0.49
CNF-TO	98.6	99.8	13.4	9.4	7.36	10.62
Ref. LBG	95.6	99.2	33.2	42.9	2.88	2.31

Similarly, temperature also influenced the biogreases' ability to recover their original structure, with this recovery capacity being strongly dependent on the type of thickener used. For instance, the "healing" index of the CNF-B biogrease declined from 52.0 to 31.0% as the temperature increased from 25 to 60 °C. Comparable reductions in the "healing" index were observed for both CNF-TO and CNF-U biogreases. However, at both temperatures, the recovery capacity of CNF-TO was significantly lower than that of CNF-B, while CNF-U demonstrated a markedly higher ability to recover. The CNF-U biogrease exhibited exceptional self-structural resilience, with its cellulose network capable of reorganizing and restoring its original structure to a considerable extent even at 60 °C. This superior structural stability is largely attributed to the intrinsic properties of unbleached cellulose nanofibers, which retain higher levels of natural lignin and hemicellulose [15]. These components act as natural fillers and cross-linking agents, reinforcing the entangled network and enhancing the biogrease's structural resistance to mechanical disruption [28]. From a practical perspective, this resilience makes CNF-U biogrease particularly suitable for applications requiring enhanced durability, load-bearing capacity, and long-term mechanical stability.

At this stage, it is important to highlight the physical origin of the instability discussed above, particularly in relation to Figure 4. According to Ovarlez et al. [29], the shear-banding phenomenon observed in complex fluids arises from the interplay between structural breakdown induced by flow and structural recovery driven by aging. In the case of CNF-TO biogrease, the combination of a high "damage" index and a low "healing" index—resulting in a markedly elevated damage/healing ratio compared to other formulations—indicates minimal competition between these two opposing structural processes. This imbalance leads to a more stable and consistent steady-state viscous flow profile across the range of shear rates and temperatures examined. In contrast, a more balanced ratio between mechanical degradation and recovery capacity may intensify the competition between these structural events, potentially giving rise to the dynamically unstable region observed during viscometric flow at moderate shear rates and elevated temperatures. From a practical perspective, the lower resistance to shear-induced damage exhibited by CNF-TO biogrease may facilitate the migration of cellulose nanofibers toward the contact interface.

Consequently, high "damage" index values tend to correlate with lower coefficients of friction under boundary and mixed lubrication regimes. Conversely, the exceptional self-structural resilience of CNF-U biogrease likely contributes to its higher coefficient of friction and the more uniform friction profile observed across the entire sliding velocity range.

In conclusion, the rheological analysis revealed significant differences in shear stability among the biogreases. While all formulations exhibited shear-thinning behavior, CNF-TO maintained a relatively stable viscosity across temperatures, attributed to its robust internal network. In contrast, CNF-U demonstrated the greatest resistance to shear-induced damage and superior self-healing capability, owing to its lignin-rich unbleached cellulose fibers. This formulation preserved its mechanical stability even at elevated temperatures (60 °C), highlighting its exceptional resilience. CNF-B and CNF-TO were more susceptible to mechanical disruption, although CNF-TO consistently maintained a stable flow profile under varying conditions. These observations underscore the critical role of microstructural resilience in shaping the tribological performance of the biogreases. Specifically, high "damage" index values—such as those observed in CNF-TO and LBG—were associated with reduced friction and improved lubricant film formation. Conversely, the outstanding structural recovery of CNF-U contributed to higher friction levels but yielded a more uniform and predictable friction profile, making it particularly well-suited for high-load, long-duration applications.

3.4. Wear Analysis of Nanocellulose-Based Biogreases

The analysis of the time-dependent evolution of the coefficient of friction (COF), along with the resulting wear scars, provided a more comprehensive tribological characterization of the CNF-based biogreases. Wear tests were conducted at both 25 and 60 °C under a normal load of 20 N and a rotational speed of 40 rpm, corresponding to a sliding velocity of 18.8 mm/s. These conditions fall within the mixed lubrication regime, where friction behavior is influenced not only by the nature of the contacting surfaces but also by lubricant viscosity, applied load, and sliding velocity [24,30]. As such, the selected parameters allowed for a realistic evaluation of the biogreases' performance under practical operating conditions, offering valuable insights into their lubrication effectiveness across different temperatures.

Figure 6a illustrates the time evolution of the COF at 25 °C under the specified load and velocity (20 N, 18.8 mm/s). Typically, the friction curve exhibited an initial transition phase—commonly referred to as the "running-in" period—likely caused by surface asperity adaptation or the formation of a lubricating film. This phase was followed by a more stable and consistent regime, representing the true steady-state behavior of the biogrease under the given tribological conditions. The shape of the friction curves suggests that the biogreases operated under fully flooded conditions, with the development of a protective lubricant film [31].

Notable differences were observed among the formulations. CNF-TO and CNF-U biogreases displayed the expected friction profile: high initial COF values due to static friction, followed by a stable dynamic friction regime with lower COF values. The presence of non-smooth curves was attributed to intermittent thickener migration across the contact zone and occasional asperity interactions—typical features of mixed lubrication [31]. In contrast, CNF-B biogrease initially exhibited lower COF values that gradually increased and stabilized at higher levels as the test progressed. This behavior has been attributed by some researchers to lubricant film breakdown due to insufficient lubricant supply [32,33], or to more severe surface damage [34]. Alternatively, it may result from the accumulation of cellulose fibrils wrapping around the tribopair surfaces, which could increase friction forces while simultaneously forming a protective surface film [12].

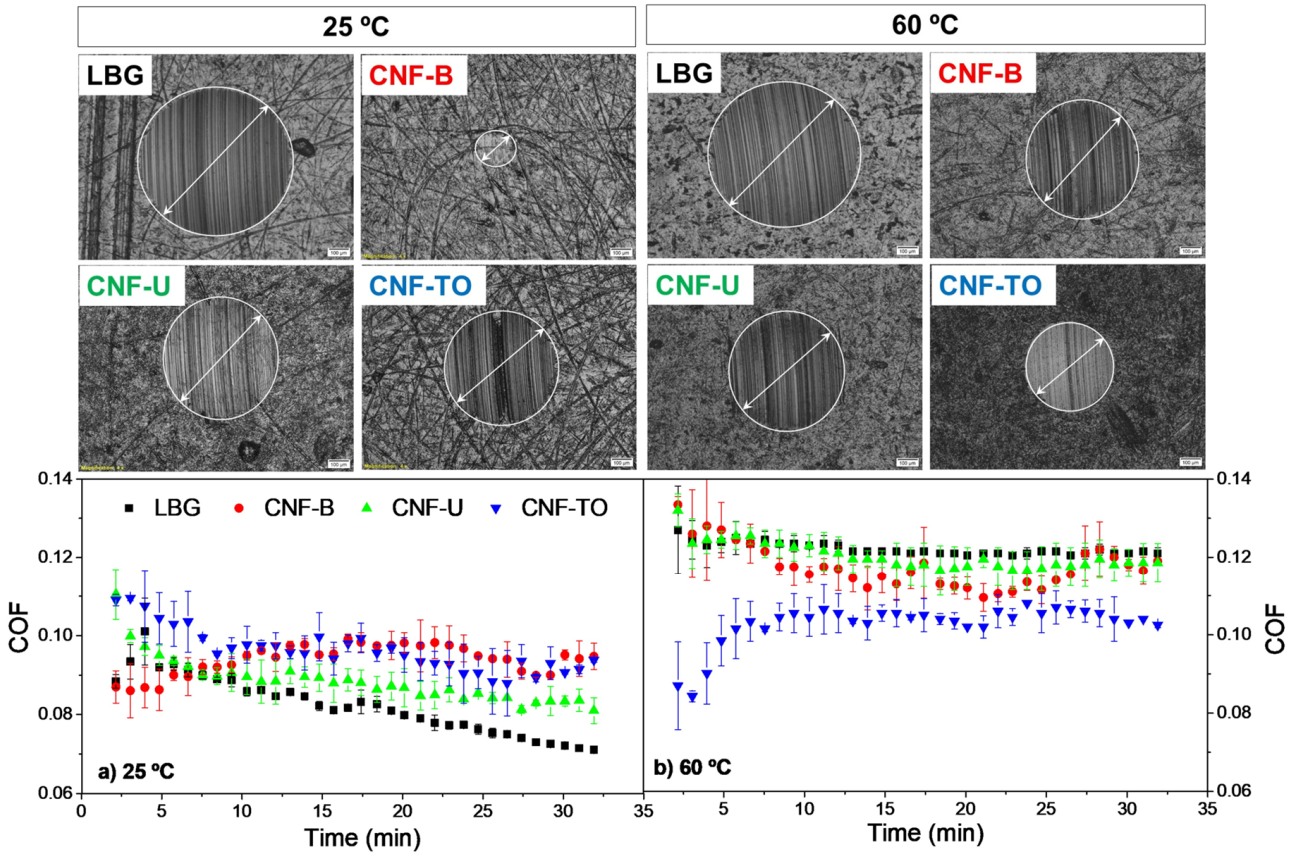

Figure 6. Variation in coefficient of friction with time during wear test at constant rotational speed of 40 rpm and normal load of 20 N at: (**a**) 25 °C; (**b**) 60 °C. Wear scars are included for all tests.

For the reference LBG, the COF slightly decreased over time, ultimately yielding significantly lower values than those observed for the CNF-based biogreases. This trend aligns with the data presented in Figure 2b, which shows the lowest COF values for LBG under the same load and temperature conditions (20 N, 25 °C).

Additionally, optical microscopy was used to visualize the wear scars formed on steel plates after testing (Figure 6), and their dimensions were subsequently evaluated (Figure 7). Rounded wear marks were observed in all cases, accompanied by numerous micro-furrow ditches across the plate surfaces. Interestingly, the reference LBG—despite exhibiting the lowest coefficients of friction at 20 N and 25 °C—produced the largest wear scar diameters (Figure 6a). This finding suggests that CNF-based biogreases form a more robust tribofilm, offering superior protection and lubrication efficiency compared to the film generated by LBG, even though both share the same base oil. The presence of cellulose nanofibrils in the tribological contact appears to effectively prevent surface degradation.

In this context, it is noteworthy that both Ilyin et al. [12] and Guimarey et al. [13] demonstrated that low concentrations of cellulose microfibrils and rod-like cellulose nanocrystals, respectively, act as fillers by penetrating and smoothing microscopic surface irregularities. This mechanism reduces wear by minimizing direct asperity contact and contributes to a self-repairing effect that enhances the smoothness of tribopair surfaces [13]. In addition to lowering wear, this process improves the mechanical stability of frictional interactions, thereby extending the lifespan of the contacting materials [12]. Special attention should be given to the biogrease formulated with bleached PFI-refined nanofibers (CNF-B), which yielded an exceptionally low wear scar diameter of 188 µm—significantly smaller than those of the other CNF-based biogreases (Figure 7). As previously discussed, CNF-B

also exhibited a distinct friction profile over time, suggesting the accumulation of cellulose fibrils around the tribopair surfaces.

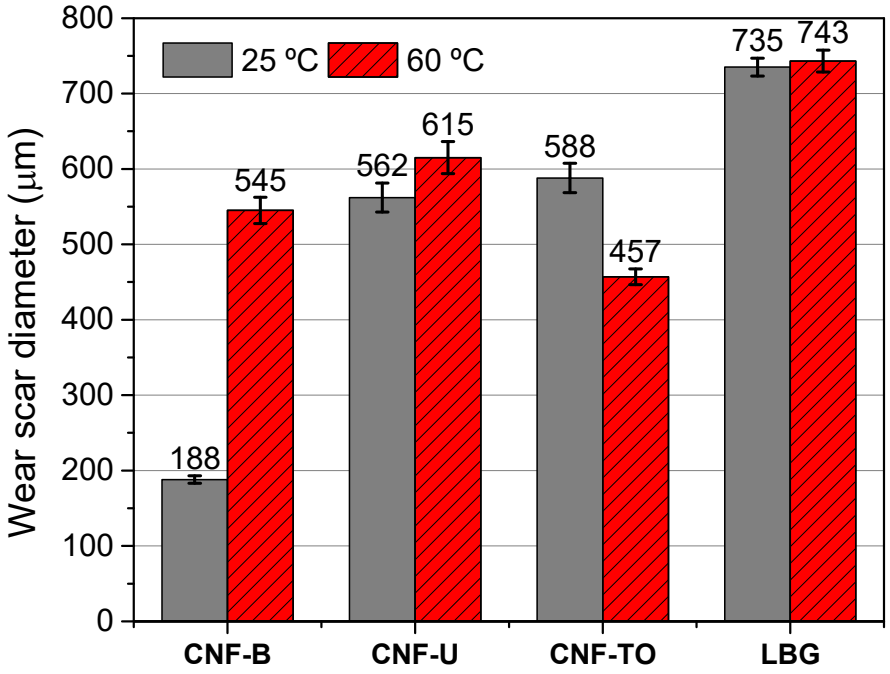

Figure 7. Comparative evaluation, at 25 and 60 °C, of scar diameters from wear tests at a constant rotational speed of 40 rpm and normal load of 20 N.

The effect of temperature was also examined. As shown in Figure 6b, higher coefficients of friction were recorded at 60 °C, accompanied by larger wear scar diameters (Figure 7). In general, both friction and wear increased with temperature, likely due to the reduction in base oil viscosity [35]. Once again, the reference LBG produced the largest wear scars, with minimal variation between 25 °C and 60 °C (735 µm and 743 µm, respectively), despite a significant increase in its friction curve at elevated temperature. The similar friction behavior observed for CNF-B and CNF-U at 60 °C resulted in comparable wear scar diameters—545 µm and 615 µm, respectively. Remarkably, CNF-TO exhibited a friction profile at 60 °C that closely resembled the behavior of CNF-B at 25 °C. Consequently, CNF-TO showed an unexpected 22% reduction in wear scar diameter, from 588 µm at 25 °C to 457 µm at 60 °C. In fact, CNF-TO yielded the smallest wear scar diameter at 60 °C among all tested greases. In summary, the wear-reducing effectiveness of CNF-based biogreases is most evident when cellulose fibrils accumulate around the tribopair surfaces during the "running-in" phase, as demonstrated by CNF-B at 25 °C and CNF-TO at 60 °C.

Finally, it is worth highlighting the comparable coefficients of friction observed at both 25 and 60 °C when the tribological contact was lubricated with the CNF-TO biogrease. Despite its known stress sensitivity, as previously discussed, the polar carboxyl groups introduced through TEMPO-mediated oxidation may facilitate stronger interactions with the steel surface. These interactions likely mitigate the influence of temperature on the formation and stability of the lubricant film.

In conclusion, wear tests confirmed that CNF-based biogreases offer superior surface protection compared to the conventional lithium-based reference grease. Notably, CNF-B at 25 °C and CNF-TO at 60 °C produced the smallest wear scar diameters, likely due to the accumulation of cellulose fibrils forming protective tribofilms. Although friction generally increased with temperature, the CNF-based formulations consistently demonstrated enhanced wear resistance, underscoring their potential as eco-friendly and high-performance lubricants.

4. Conclusions

The nanocellulose-based biogreases investigated in this study consistently outperformed the reference lithium soap grease. The influence of temperature on the thickener's structural resistance to mechanical disruption and its frictional behavior was notably less pronounced in the nanocellulose formulations. This suggests that superior performance can be achieved with lower thickener concentrations and more sustainable raw materials, thereby confirming our first hypothesis.

The pulp bleaching process played a significant role in determining tribological outcomes. The biogrease derived from unbleached nanofibers, which contained the highest lignin content (~2.6 wt.%), exhibited the highest coefficient of friction across the entire range of sliding velocities tested. Nanofibrillation pretreatment also proved critical: chemically treated nanofibers demonstrated exceptional friction-reducing capabilities and optimal tribological performance across diverse lubrication regimes. Their lower resistance to shear-induced damage may have facilitated the penetration of nanofibers into the contact zone. Furthermore, the polar carboxyl groups introduced via TEMPO-mediated oxidation likely enhanced interactions with the steel surface. The relatively small wear scar diameter observed at 60 °C underscores the potential of this nanofiber as an additive for high-temperature applications.

Particular attention should be given to the initial accommodation phase of nanofibers, which proved highly effective in reducing wear. This phase was marked by lower coefficients of friction that gradually increased and stabilized as the test progressed. The phenomenon is attributed to the accumulation of cellulose fibrils wrapping the tribopair surfaces—a conclusion supported by the exceptionally small wear scar diameter observed at 25 °C when lubricated with biogrease derived from bleached mechanical nanofibers.

Overall, these findings, which confirm our second hypothesis, underscore the importance of tailoring nanocellulose formulations to the mechanical demands of specific applications. Chemically treated and bleached mechanical nanofibers are better suited for environments with moderate shear stress, while unbleached mechanical nanofibers are ideal for conditions requiring resilience to significant mechanical deformation.

Despite the promising results, this study was conducted under controlled laboratory conditions. Nevertheless, the high performance and structural robustness of CNF-based biogreases indicate strong potential for real-world applications in environmentally sensitive sectors such as wind energy, agricultural machinery, and marine systems. Future research will focus on scaling up these formulations, conducting field trials, and performing comprehensive life cycle and biodegradability assessments to validate their industrial viability.

Author Contributions: C.R.: conceptualization, methodology, writing—original draft, validation, and investigation; M.Á.D.C.: conceptualization, methodology, resources, writing—review and editing, project administration, and funding acquisition; M.G.-P.: methodology, validation, and investigation; S.D.F.-S.: methodology, validation, and investigation; K.L.: Validation and writing—review and editing; M.G.-M.: conceptualization, methodology, writing—review and editing, supervision, project administration, and funding acquisition; All authors have read and agreed to the published version of the manuscript.

Funding: This work is part of the "Programa Operativo FEDER-Andalucía 2021-27: Applied Research (call 2023)" project (EPIT1312023) co-funded by UE-Ministerio de Hacienda y Función Pública–Fondos Europeos–Consejería de Universidad, Investigación e Innovación. Funding for open access publishing: Universidad de Huelva/CBUA.

Data Availability Statement: The data that support the findings of this study are available from the corresponding author upon reasonable request.

Acknowledgments: During the preparation of this work the author used MS Copilot with GPT-4 for text to improve language and readability of the manuscript. After using this tool/service, the author reviewed and edited the content as needed and takes full responsibility for the content of the publication.

Conflicts of Interest: The authors declare no conflicts of interest.

References

1. Kowalski, J.; Leśniewski, W.; Piatek, D.; Cuper, D. Assessing the Potential Replacement of Mineral Oil with Environmentally Acceptable Lubricants in a Stern Tube Bearing: An Experimental Analysis of Bearing Performance. *Pol. Marit. Res.* **2021**, *28*, 160–166. [CrossRef]
2. Nifant'ev, I.E.; Vinogradov, A.A.; Vinogradov, A.A.; Bagrov, V.V.; Churakov, A.V.; Minyaev, M.E.; Kiselev, A.V.; Salakhov, I.I.; Ivchenko, P.V. A competitive way to low-viscosity PAO base stocks via heterocene-catalyzed oligomerization of dec-1-ene. *Mol. Catal.* **2022**, *529*, 112542. [CrossRef]
3. Rajewski, T.E.; Fokens, J.S.; Watson, M.C. The development and application of synthetic food grade lubricants. *Ind. Lubr. Tribol.* **2000**, *52*, 110–116. [CrossRef]
4. Sánchez, R.; Franco, J.M.; Delgado, M.A.; Valencia, C.; Gallegos, C.J. Rheological and mechanical properties of oleogels based on castor oil and cellulosic derivatives potentially applicable as bio-lubricating greases: Influence of cellulosic derivatives concentration ratio. *Ind. Eng. Chem.* **2011**, *17*, 705–711. [CrossRef]
5. Sánchez, R.; Fiedler, M.; Kuhn, E.; Franco, J.M. Tribological characterization of green lubricating greases formulated with castor oil and different biogenic thickener agents: A comparative experimental study. *Ind. Lubr. Tribol.* **2011**, *63*, 446–452. [CrossRef]
6. Borrero-López, A.M.; Martín-Sampedro, R.; Ibarra, D.; Valencia, C.; Eugenio, M.E.; Franco, J.M. Evaluation of lignin-enriched side-streams from different biomass conversion processes as thickeners in bio-lubricant formulations. *Int. J. Biol. Macromol.* **2020**, *16*, 1398–1413. [CrossRef]
7. Borrero-López, A.M.; Valencia, C.; Franco, J.M. Lignocellulosic Materials for the Production of Biofuels, Biochemicals and Biomaterials and Applications of Lignocellulose-Based Polyurethanes: A Review. *Polymers* **2022**, *14*, 881. [CrossRef]
8. Mu, L.; Wu, J.; Matsakas, L.; Chen, M.; Vahidi, A.; Grahn, M. Lignin from Hardwood and Softwood Biomass as a Lubricating Additive to Ethylene Glycol. *Molecules* **2018**, *23*, 537. [CrossRef]
9. Taha, M.; Mousa, H.M.; Alfadhel, H.; Abouel Nasr, E.; Elbatran, A.H.A.; Nabhan, A.; El-Sharkawy, M.R. Utilizing cellulose nanofibers to enhance spent engine oil performance: A sustainable environmental solution. *Results Eng.* **2024**, *23*, 102395. [CrossRef]
10. Awang, N.W.; Ramasamy, D.; Kadirgama, K.; Samykano, M.; Najafi, G.; Che Sidik, N.A. An experimental study on characterization and properties of nano lubricant containing cellulose nanocrystal (CNC). *Int. J. Heat Mass Transf.* **2019**, *130*, 1163–1169. [CrossRef]
11. Li, J.; Lin, N.; Du, C.; Ge, Y.; Amann, T.; Feng, H.; Yuan, C.; Li, K. Tribological behavior of cellulose nanocrystal as an eco-friendly additive in lithium-based greases. *Carbohydr. Polym.* **2022**, *290*, 119478. [CrossRef] [PubMed]
12. Ilyin, S.O.; Gorbacheva, S.N.; Yadykova, A.Y. Rheology and tribology of nanocellulose-based biodegradable greases: Wear and friction protection mechanisms of cellulose microfibrils. *Tribol. Int.* **2023**, *178*, 108080. [CrossRef]
13. Guimarey, M.J.G.; Marcos, M.A.; Vallejo, J.P.; Viesca, J.L.; Comuñas, M.J.P.; Lugo, L.; Hernández Battez, A. Improving tribological efficiency of isopropyl palmitate oil with cellulose nanocrystals: A sustainable approach for high-performance lubricants. *Cellulose* **2024**, *31*, 10879–10894. [CrossRef]
14. Roman, C.; García-Morales, M.; Eugenio, M.E.; Ibarra, D.; Martín-Sampedro, R.; Delgado, M.A. A sustainable methanol-based solvent exchange method to produce nanocellulose-based ecofriendly lubricants. *J. Clean. Prod.* **2021**, *319*, 128673. [CrossRef]
15. Roman, C.; Delgado, M.A.; Fernández-Silva, S.D.; García-Morales, M. Green oleogels based on elm pulp cellulose nanofibers: Effect of the nanofibrillation pre-treatment on their thermo-rheological behavior. *Cellulose* **2024**, *31*, 321–333. [CrossRef]
16. Delgado, M.A.; Valencia, C.; Sánchez, M.C.; Franco, J.M.; Gallegos, C. Thermorheological behaviour of a lithium lubricating grease. *Tribol. Lett.* **2006**, *23*, 47–54. [CrossRef]
17. Heyer, P.; Läuger, J. Correlation between friction and flow of lubricating greases in a new tribometer device. *Lubr. Sci.* **2009**, *21*, 253–268. [CrossRef]
18. Arbella Feliciano, Y.; Trinchet Varela, C.A.; Vargas Guativas, J.A.; Lorente-Leyva, L.L.; Peluffo-Ordóñez, D.H. Evaluation of Working Temperature in Wind Turbine Bearings by Simulation of Lubricant Level. *Int. J. Des. Nat. Ecodynamics* **2021**, *16*, 99–104. [CrossRef]
19. Chatra, S.; Lugt, P.M. The process of churning in a grease lubricated rolling bearing: Channeling and clearing. *Tribol. Int.* **2021**, *153*, 106661. [CrossRef]
20. Peng, H.; Li, S.; Shangguan, L.; Zhang, H.; Zhao, D. Research on the Rheological Characteristics of Wind Power Grease Based on Rheological Parameters. *Lubricants* **2023**, *11*, 299. [CrossRef]

21. Li, H.; Zeng, Q.; Fan, M.; Pang, Z.; Wang, J.; Liang, Y. Recent progress in high-temperature greases: Constitutive relationships, mechanisms, and applications. *Friction* **2025**, *13*, 9440951. [CrossRef]
22. Cann, P.M. Grease lubrication of rolling element bearings—Role of the film thickness. *Lubr. Sci.* **2007**, *19*, 183–196. [CrossRef]
23. Wang, J.; Zhang, H.; Hu, W.; Li, J. Tribological Properties and Lubrication Mechanism of Nickel Nanoparticles as an Additive in Lithium Grease. *Nanomaterials* **2022**, *12*, 2287. [CrossRef] [PubMed]
24. Brandão, J.A.; Meheux, M.; Ville, F.; Seabra, J.H.O.; Castro, J.; Castro, *J*. Comparative overview of five gear oils in mixed and boundary film lubrication. *Tribol. Int.* **2012**, *47*, 50–61. [CrossRef]
25. Kuhn, E. Tribological Stress of Lubricating Greases in the Light of System Entropy. *Lubricants* **2016**, *74*, 37. [CrossRef]
26. Britton, M.M.; Callaghan, P.T. Two-Phase Shear Band Structures at Uniform Stress. *Phys. Rev. Lett.* **1997**, *78*, 4930. [CrossRef]
27. Delgado, M.A.; Secouard, S.; Valencia, C.; Franco, J.M. On the Steady-State Flow and Yielding Behaviour of Lubricating Greases. *Fluids* **2019**, *4*, 6. [CrossRef]
28. Liao, J.J.; Latif, N.H.A.; Trache, D.; Brosse, N.; Hussin, M.H. Current advancement on the isolation, characterization and application of lignin. *Int. J. Biol. Macromol.* **2020**, *162*, 985–1024. [CrossRef]
29. Ovarlez, G.; Rodts, S.; Chateau, X.; Coussot, P.; Coussot, *P*. Phenomenology and physical origin of shear localization and shear banding in complex fluids. *Rheol. Acta* **2009**, *48*, 831–844. [CrossRef]
30. Biresaw, G.; Bantchev, G.J. Effect of chemical structure on film-forming properties of seed oils. *Synth. Lubric.* **2008**, *25*, 159–183. [CrossRef]
31. Cousseau, T. Grease Lubrication: Formulation Effects on Tribological Performance. In *Tribology of Machine Elements—Fundamentals and Applications*; Pintaude, G., Cousseau, T., Rudawska, A., Eds.; IntechOpen, 2022. Available online: https://www.intechopen.com/chapters/79676 (accessed on 17 September 2025). [CrossRef]
32. Alp, A.; Erdemir, A.; Kumar, S. Energy and wear analysis in lubricated sliding contactions. *Wear* **1996**, *191*, 261–264. [CrossRef]
33. Begelinger, A.; De Gee, A.W. Failure of thin film lubrication—A detailed study of the lubricant film breakdown mechanism. *Wear* **1982**, *77*, 57–63. [CrossRef]
34. Nagît, G.; Mihalache, A.M.; Dodun, O.; Hrituc, A.; Slatineanu, L.; Merticaru, V. Change in Time of the Value of Dry and Lubricated Friction Coefficients for Surfaces Generated by Different Processing Methods. *Lubricants* **2023**, *11*, 436. [CrossRef]
35. Cai, Z.; Zhou, B.; Qu, Y. Effect of oil temperature on tribological behavior of a lubricated steel−steel contact. *Wear* **2015**, *332*, 1158–1163. [CrossRef]